Build Control Command Set Based on EEG Signals via Clustering Algorithm and Multi-Layer Neural Network

Quang Chuyen Lam[1], Luong Anh Tuan Nguyen[2], and Huu Khuong Nguyen[2]
[1] Ho Chi Minh City Industry and Trade College, Vietnam
[2] Ho Chi Minh City University of Transport, Viet Nam
Email: lamquangchuyen@gmail.com; {nlatuan, nhkhuong}@hcmutrans.edu.vn

Abstract —Electroencephalography (EEG) is an electrophysiological monitoring method to record electrical activity of the brain. EEG-based control is increasingly being discovered by many researchers aims to support disabled people. In order to build control command set, the system will classify the EEG signal received of user looking at the different types of images. The good results of EEG signal classification will help make control more effectively. In this paper, a novel approach proposes the classification of EEG signals based on Wavelet transform, K-means clustering algorithm and Multi-Layer Neural Network. The system architecture was designed and evaluated with the dataset of 21,000 samples. The best accuracy rate can obtain 93.57 %.

Index Terms—EEG signals, wavelet transform, K-means, neural network

I. Introduction

Brain-Computer Interface (BCI) is a new technology based on EEG signals [1] that provides a new way for the elderly and disabled people communicate with the outside world.

The aim of Brain-Computer Interface research is to establish a new augmented communication system that translates human intentions into a control signal for an output device such as a computer application or a neuroprosthesis [2].

The strength of BCI applications lies in the way we translate the neural patterns extracted from EEG signals into computer commands. EEG signal analysis was applied in medicine such as early detection of Alzheimer [3], epilepsy [4], etc. and applied in telecommunication such as calling or listening music based on EEG brain signal [5]. In these recent years, EEG-based control systems are more interested by researchers. However, the result of EEG signal identification must be very good, the controlling based on EEG signal will be better. The previous studies classifying EEG signals based on eye blink [6], eye movement [7] or head movement [8].

This paper is developed from our previous work [9]. The purpose of this paper is to classify EEG signals into 5 classes with the images user looking at such as animal images, landscape images, city images, human images and flower images. From five signal classes, five control commands were formed respectively. Fig. 1 depicts images classified into 5 classes. Fig. 2 depicts five control commands corresponding to five image classes in Fig. 1. The proposed technique uses Mexican hat Wavelet transform for signal denoising and for feature extraction, then using K-means method to cluster and multi-layer neural network to classify. Furthermore, this method also only select a few channels to process aims to reduce the execution time.

The rest of the paper is structured as follows. Section 2 provides the theoretical background in term of EEG. The system architecture and datasets are described in detail of Section 3. Section 4 presents the results from experiments and discussion. Section 5 gives conclusions and outlines future research directions.

Fig. 1. Images classified into 5 classes.

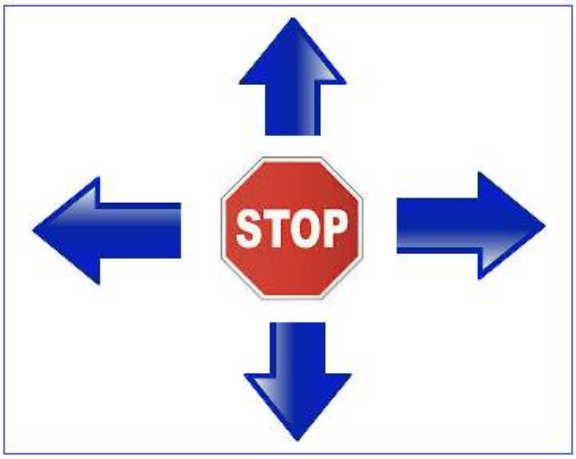

Fig. 2. Five control commands.

Manuscript received January 24, 2018; revised June 22, 2018.
Corresponding author email: nlatuan@hcmutrans.edu.vn
doi:10.12720/jcm.13.7.406-413

II. EEG Theoretical Background

A. EEG Signals

The characteristic of EEG signals is constantly changing with the frequency from 0 - 100Hz. Fig. 3 shows recorded EEG signal. EEG signals are recorded by electrode cap or headset with different channels such as 14-channel, 16-channel, 32-channel, 64-channel, etc.

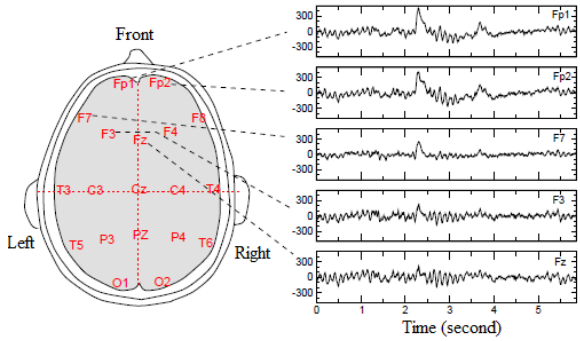

Fig. 3. Description of recorded EEG signal.

B. EEG Devices

EEG devices are divided into two main categories including EEG cap and EEG headset. Figure 4 describes the EEG cap used for recording EEG signals and Figure 5 describes the EEG headset.

Fig. 4. Electrode cap.

Fig. 5. EEG headset.

C. EEG Bands

EEG signal is divided into 5 types of wave as follows: delta (1-4 Hz), theta (4-8 Hz), alpha (8-13 Hz), beta (13-30 Hz) and gamma (30-100 Hz) [10].

Delta is the frequency range up to 4Hz. It tends to be the highest in amplitude and the slowest waves. It is seen normally in adults in slow-wave sleep. It is also seen normally in babies. It may occur focally with subcortical lesions and in general distribution with diffuse lesions, metabolic encephalopathy hydrocephalus or deep midline lesions. It is usually most prominent frontally in adults (e.g. FIRDA – frontal intermittent rhythmic delta) and posteriorly in children (e.g. OIRDA – occipital intermittent rhythmic delta) [11]. Fig. 6 depicts delta waves.

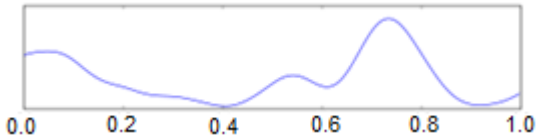

Fig. 6. Delta Waves.

Theta is the frequency range from 4Hz to 8Hz. Theta is seen normally in young children. It may be seen in drowsiness or arousal in older children and adults; it can also be seen in meditation [12]. Fig. 7 depicts theta waves.

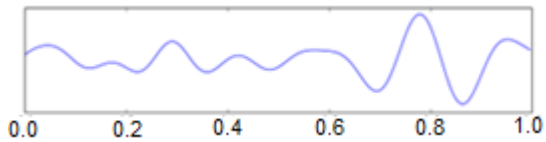

Fig. 7. Theta Waves.

Alpha is the frequency range from 8 Hz to 13 Hz. Hans Berger named the first rhythmic EEG activity he saw as the "alpha wave". This was the "posterior basic rhythm" (also called the "posterior dominant rhythm" or the "posterior alpha rhythm"), seen in the posterior regions of the head on both sides, higher in amplitude on the dominant side [13]. Fig. 8 depicts alpha waves.

Fig. 8. Alpha waves.

Beta is the frequency range from 13 Hz to about 30 Hz. It is seen usually on both sides in symmetrical distribution and is most evident frontally. Beta activity is closely linked to motor behavior and is generally attenuated during active movements [14]. Fig. 9 depicts beta waves.

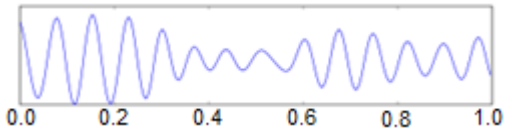

Fig. 9. Beta waves.

Gamma is the frequency range approximately 30–100Hz. Gamma rhythms are thought to represent binding of different populations of neurons together into a network for the purpose of carrying out a certain

cognitive or motor function [15]. Fig. 10 depicts gamma waves.

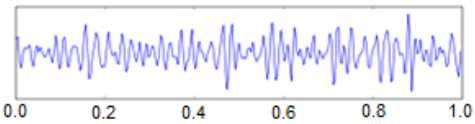

Fig. 10. Gamma waves.

III. Materials and Methods

A. Data Acquisition

The experimental dataset was taken from [16]. The data collected from some volunteer participants as follows: The participants wear hat with recording 32-channels EEG signals and sit in front of a computer screen about 110cm, they perform two tasks alternately: classification and identification. The participants will perform in two days: the first day including 11 persons perform and the second day including 10 persons perform. Each person performs 1,000 images for one task.

To start work, the participant will press and hold the touch button. An 8-bit color image (256 pixels of width and 256 pixels of height) appears in about 200ms, the participant will release the button if the image is target image. The first period of 1000ms is considered the reaction time of the participant, the total time for an experimental image is 2000 ±200ms described in Fig. 9.

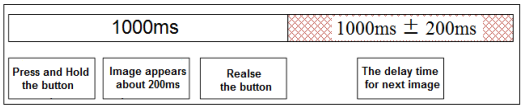

Fig. 11. The schema for an image.

B. Channels Selection

Many of the EEG channels appeared to represent redundant information. This mean that there is no need to analyze all 32 channels.

According to [17], only ten electrode locations are commonly used such as F3, C3, P3, O1, F4, C4, P4, O2, A1 and A2. In this paper, the proposed method used these channels instead of 32 channels for experimentation. The 32-channel EEG signal is depicted in Fig. 10.

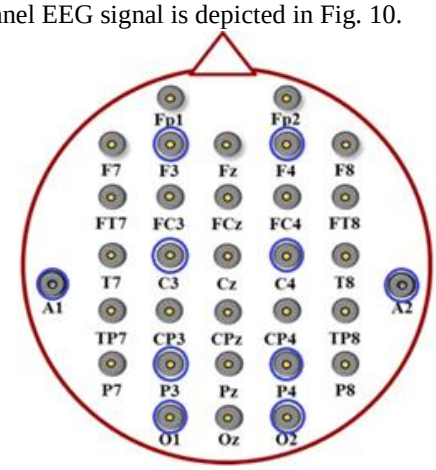

Fig. 12. Electrodes of 32-Channel EEG signal

C. System Architecture

The system architecture including 4 phase is presented in Fig. 13.

- The first phase: selecting 10 electrode locations commonly used such as F3, C3, P3, O1, F4, C4, P4, O2, A1 and A2.
- The second phase: Wavelet Transform is used for feature extraction and noise reduction.
- The third phase: Clustering algorithm is used to group into 5 clusters such as Delta, Theta, Alpha, Beta and Gamma.
- The forth phase: The multi-layer neural network including 5 input nodes (delta, theta, alpha, beta and gamma), one hidden layer with respect to variations in number of neurons and one output node used for determining the result of classification.

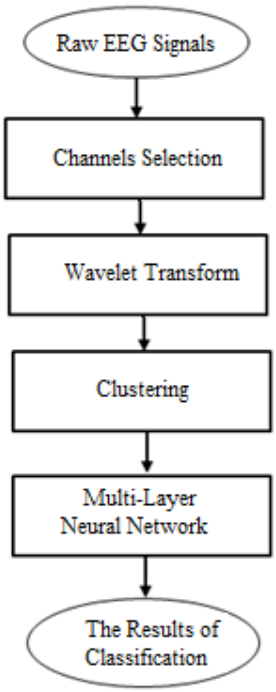

Fig. 13. System architecture

D. Wavelet Transform

Raw EEG signals suffer from poor spatial resolution, low signal-to-noise ratio and artifacts [18]. Wavelet Transform is used for signal denoising and for feature extraction. Wavelet Transform was developed in the 1980s as a powerful signal processing technique to overcome the shortcomings of other methods such as the Fourier transform [19]. Wavelet Transform acts like a mathematical microscope, because it has the capability to analyze EEG signals at different scales [20]. Wavelet Transform is now a well-known tool for removing noise from the signal. Multi-resolution analysis provides information about the signal in different frequency bands.

In this paper, *Mexican hat* Wavelet transform is used for feature extraction and noise reduction by (1) and (2) [21].

$$W(a,b)=\frac{1}{\sqrt{a}}\int_{-\infty}^{\infty}x(t)\psi^{*}\left(\frac{t-b}{a}\right)dt \tag{1}$$

$$\psi(t)=\frac{2}{\pi^{1/4}\sqrt{3}}(1-t^{2})e^{-t^{2}/2} \tag{2}$$

where, *x(t)* is the signal at interval *a* and time *b*. *Mexican hat* Wavelet is illustrated in Fig. 14.

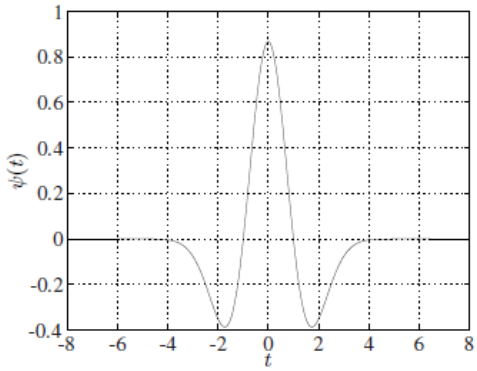

Fig. 14. *Mexican hat* Wavelet.

E. K-Means Clustering

Clustering method divides a dataset into groups according to similarities or dissimilarities among the patterns. K-means algorithm is one of the simplest and well known clustering algorithms [22].

This algorithm determines the cluster centers and the elements belonging to them by minimizing the squared error based objective function. The aim of the algorithm is to locate the cluster centers as much as possible far away from each other and to associate each data point to the nearest cluster center. Euclidean distance is usually used as the dissimilarity measure in K-means algorithm. The objective function J is described as follows:

$$J=\sum_{i=1}^{K}\left(\sum_{k}\|x_k-c_i\|^2\right) \tag{3}$$

where, K is the number of clusters, c_i is the centers of clusters, and x_k is k^{th} data point in i^{th} cluster. A data point belongs to a cluster whose center is the closest to that data point. Thus, the clusters are represented by binary membership matrix U. The elements of matrix U are determined as follows:

$$u_{ij}=\begin{cases}1 & \text{if } \|x_j-c_i\|^2\leqslant\|x_j-c_t\|^2,\ \forall t\neq i\\ 0 & \text{otherwise}\end{cases} \tag{4}$$

where, u_{ij} shows that j^{th} data point belongs to i^{th} cluster, or not. Each cluster center c_i minimizing the objective function J is defined as follows:

$$c_i=\frac{\sum_{j=1}^{N}u_{ij}x_j}{\sum_{j=1}^{N}u_{ij}} \tag{5}$$

where, N is the number of data points. The algorithm is shown in Fig. 15 [23]:

Repeat

// Computing the membership matrix U by (4)

$$u_{ij}=\begin{cases}1 & \text{if } \|x_j-c_i\|^2\leqslant\|x_j-c_t\|^2,\ \forall t\neq i\\ 0 & \text{otherwise}\end{cases}$$

// Calculating the objective function J by (3)

$$J=\sum_{i=1}^{K}\left(\sum_{k}\|x_k-c_i\|^2\right)$$

// Updating the positions of the cluster centers by (5)

$$c_i=\frac{\sum_{j=1}^{N}u_{ij}x_j}{\sum_{j=1}^{N}u_{ij}}$$

Until (The cluster centers no longer move)

Fig. 15. K-means algorithm.

In this paper, K=5 is used to group into 5 clusters such as Delta, Theta, Alpha, Beta and Gamma.

F. Multi-Layer Neural Network

Artificial neural network (ANN) is a mathematical model that mimics some functional aspects of biological neuron network. Usually ANN has one input layer, one output layer and one or more hidden neuron layers. Theoretically network with one hidden layer of neurons can solve task of any complexity [24]. The multi-layer neural network model including 3 layers is presented in Fig. 16.

The first layer contains five nodes such as delta, theta, alpha, beta and gamma. This layer is called the input layer.

The second layer is the hidden layer. The number of neurons in hidden layer was set to 5, 10, 15, 20, 25, 30, 35, 40, 45 and 50.

The output layer contains one node, the results of this node are used to classify EEG signal. Due to the action function used in this model is hyperbolic tangent function, the value of the output node ranges in the interval [-1, 1]. Fig. 17 shows the output result.

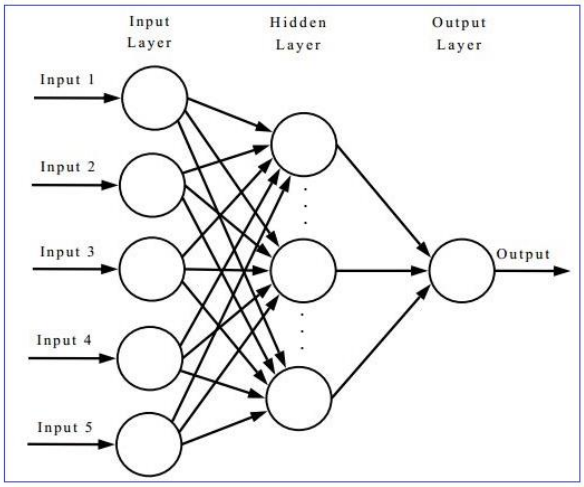

Fig. 16. Multi-Layer neural network.

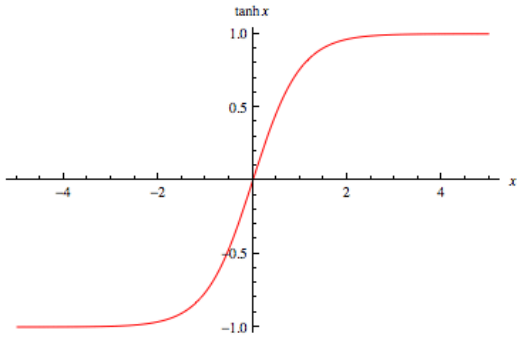

Fig. 17. Hyperbolic tangent function

Before using the model, the neural network need to pass the training phase to learn. The flow of the training algorithm is shown in Fig. 18, representing a backpropagation learning procedure [25].

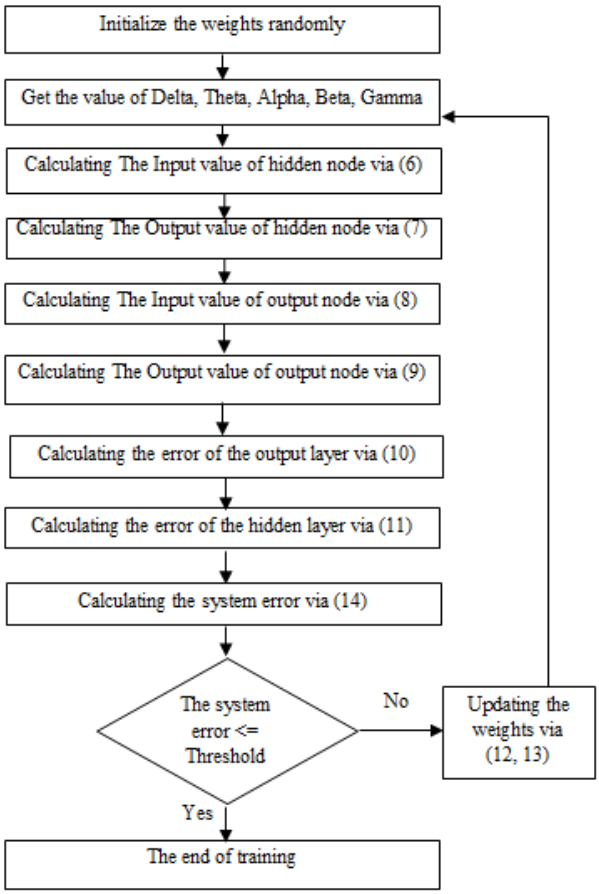

Fig. 18. Training algorithm

Entering pairs of input and output values from the training data set, this procedure iteratively propagates values from the input layer to output layer and updates the weights from the input layer to the output layer until the error of the output node is lower than the threshold.

The training algorithm performs two phases as follows:

- The "***propagation***" phase calculates the input value, the output value of each node in the hidden layer and the output layer.
  - The input value of the hidden nodes is calculated by equation (6).

$$I_i = \sum_{i=1}^{K} w_{ji} * V_j \quad ; j = 1...5 \tag{6}$$

where, I_i, V_j and w_{ji} are the ith input value of the hidden layer, the jth value of the input layer and the weight from the jth node of the previous layer to the ith node of the next layer respectively.

- The output value of the hidden nodes is calculated by equation (7).

$$O_i = \frac{1}{1+e^{-I_i}} \; ; i = 1..K \tag{7}$$

where, I_i and O_i are the ith input value and the ith output value in the hidden layer respectively.

- The input value of the output node is calculated by equation (8).

$$I = \sum_{i=1}^{K} W_i * O_i \tag{8}$$

where, O_i and W_i are the ith output value of the hidden layer and the weigh from the ith node of the hidden layer to the output node respectively.

- The output value of the output node is calculated by equation (9).

$$O = \frac{e^{I} - e^{-I}}{e^{I} + e^{-I}} \tag{9}$$

where, O and I the input value and the output value in the output layer respectively.

- The "**weight update**" phase calculates the error of the nodes in the hidden layer and the output layer, then updates the weights.
  - The error of the output node is calculated by equation (10).

$$Err = O * (1 - O) * (T - O) \tag{10}$$

where, T and O are the real value of sample in training dataset, the output value of output node respectively.

- The error of the ith node in the hidden layer is calculated by equation (11).

$$Err_i = O_i * (1 - O_i) * \sum Err * w_i \quad ; i = 1...K \tag{11}$$

where, O_i, W_i and Err are the output value of the ith hidden node, the weight of the connection from the ith hidden node to the output node and the error of the output node respectively.

- The weights from the hidden layer to the output layer are updated by equation (12).

$$\begin{cases} \Delta w_i = R. * Err * O_i \\ w_i = w_i + \Delta w_i \;\; ; \;\; i = 1...K \end{cases} \tag{12}$$

where, O_i, Err and R are the ith output value of the hidden layer, the error of the output node and the learning rate respectively.

- The weights from the input layer to the hidden layer are updated by equation (13).

$$\begin{cases} \Delta w_{ji} = R * Err_i * V_j \\ w_{ji} = w_{ji} + \Delta w_{ji} \; ; \; i = 1...K, \; j = 1...5 \end{cases} \quad (13)$$

where, V_j, Err_i and R are the jth input value, the error of the ith hidden node and the learning rate respectively.

- The system error based on RMSE [26] is calculated by equation (14).

$$Err_S = \sqrt{\frac{\sum_{i=1}^{N} (Err)^2}{N}} \quad (14)$$

where, N and Err are the number of samples in the training data set and the error of the output node respectively.

IV. Results and Discussion

Dataset including 21,000 samples was divided into subsets for training (70%), validation (15%) and testing (15%). The system uses Matlab and EEGLab toolbox for experimental process, the neural network is divided into two experimental phases:

The training phase is performed on the training subset using different topologies of neural network with respect to variations in number of neurons in hidden layer via the following parameters as follows:

- Learning rate: 0.7
- Number of epochs: 5,000
- Initializing weights random values from 0 to 1
- Mean error threshold value: 10^{-5} and based on RMSE (Root Mean Square Error).

The classification accuracy is measured as a ratio of false results to the total number of samples.

$$Error = \frac{n - n_{true}}{n} \quad (15)$$

where, n is the total number of samples, n_{true} is the number of samples with correct classification result.

Table I: Results of Experiment

No. of hidden neurons	Average Error	Minimum Error	Accuracy Rate
5	25.21%	21.98%	78.02%
10	23.77%	20.04%	79.96%
15	20.44%	17.13%	82.87%
20	17.76%	14.21%	85.79%
25	15.43%	11.88%	88.12%
30	12.98%	10.06%	89.94%
35	9.87%	7.74%	92.26%
40	**7.74%**	**6.43%**	**93.57%**
45	9.56%	7.92%	92.08%
50	10.24%	8.63%	91.37%

One can observe in Table I that classification results of test subset are constantly increasing until the best possible value (40 hidden neurons) is achieved (The best accuracy rate of 93.57%). Afterwards results start to decrease, when the number of neurons increases. This occurrence is called overfitting. Overfitting is a phenomenon when a neural network gets very good at dealing with one data set at the expense of becoming very bad at dealing with other datasets.

A confusion matrix [27] contains information about actual and predicted classifications done by a classification system. Performance of such systems is commonly evaluated using the data in the matrix. Fig. 19 depicts the performance of system evaluated by the data in the confusion matrix with 40 hidden nodes in the hidden layer .

		Actual Class				
		Animals	Landscapes	Cities	Humans	Flowers
Predicted Class	Animals	93.8%	1.4%	1.5%	2.0%	1.6%
	Landscapes	1.1%	93.6%	3.1%	1.5%	1.2%
	Cities	1.6%	1.3%	93.5%	1.6%	1.8%
	Humans	1.9%	1.8%	1.3%	93.2%	1.7%
	Flowers	1.7%	1.9%	0.8%	1.8%	93.8%

Fig. 19. Illustration of confusion matrix for the result of classification.

In order to provide a more intuitive and easier-to-understand method to measure the prediction quality, the following equation set is used in the literature for examining performance quality.

The *accuracy* (*AC*) is the proportion of the total number of predictions that were correct. It is determined using the equation (16).

$$AC = \frac{TP + TN}{TP + FP + TN + FN} \quad (16)$$

The *precision* (*P*) is the proportion of the predicted positive cases that were correct, as calculated using the equation (17).

$$p = \frac{TP}{TP + FP} \quad (17)$$

where, True positives (TP) refers to the positive tuples that were correctly labeled by the classifier. True negatives (TN) refers to the negative tuples that were correctly labeled by the classifier. False positives (FP) refers to the negative tuples that were incorrectly labeled as positive. False negatives (FN) refers to the positive tuples that were mislabeled as negative.

The success rates obtained by the testing with 40 hidden nodes in the hidden layer are given in Fig. 20.

	TP	TN	FP	FN	AC	P
Animals	93.8%	93.6%	6.4%	6.2%	93.7%	93.6%
Landscapes	93.6%	93.2%	6.8%	6.4%	93.4%	93.2%
Cities	93.5%	93.8%	6.3%	6.6%	93.6%	93.7%
Humans	93.2%	93.4%	6.6%	6.8%	93.3%	93.4%
Flowers	93.8%	93.9%	6.1%	6.2%	93.9%	93.9%

Fig. 20. The results of the testing.

These results are also compared to some previous studies such as the technique [9] obtained the best rate of 92.68%, the technique [6] identify EEG signals based on blink with 15,360 samples and reach 90.85%, the technique [7] with the decision tree achieving a maximum of 85% , the technique [8] based on eye movement by 2 experiments with 3,600 samples and 8,320 samples and reach 85%. We found that the proposed technique classifies better. Moreover, the proposed technique may apply for people with weak eye muscles or people with one eye.

V. Conclusions

The proposed method classifies EEG signals based on recorded signal when looking at images such as landscape images, animal images, city images, human images, flower images by using Mexican hat Wavelet transform, K-means clustering algorithm and multiple-layer neural network. The proposed technique was experimented with 21,000 samples via MatLab and EEGLab toolbox, the best achieved result is 93.57% with 40 hidden nodes in the hidden layer.

In the near future, we will develop the proposed method on real-time systems with Emotiv's EEG device. In addition, we will adjust the parameters of the neural network to achieve optimal performance that meets the requirements of the real-time system.

Acknowledgment

The authors wish to thank the authors of EEG dataset which is publicly available at http://sccn.ucsd.edu/~arno/fam2data/publicly_available_EEG_data.html

The authors also thank reviewers for their reading of our manuscript and their insightful comments and suggestions.

References

[1] J. R. Wolpaw, N. Birbaumer, W. J. Heetderks et al., “Brain-computer interface technology: a review of the first interna-tional meeting,” *IEEE Transactions on Rehabilitation Engineering*, vol. 8, no. 2, pp. 164–173, 2000.

[2] J. R. Wolpaw, N. Birbaumer, D. J. McFarland, G. Pfurtscheller, and T. M. Vaughan, “Brain-computer interfaces for communication and control,” *Clin. Neurophysiol*, vol. 113, pp. 767–791, 2002.

[3] Hornero, *et al.*, “Nonlinear analysis of electroencephalogram and magnetoencephalogram recordings in patients with Alzheimer’s disease,” *Phil. Trans. R. Soc. A*, vol. 367, pp. 317–336, 2009.

[4] S. J. M. Smith, “EEG in the diagnosis, classification, and management of patients with epilepsy,” *Journal of Neurol Neurosurg and Psychiatry*, vol. 76, pp. ii2-ii7, 2005.

[5] Demo-Video. Neurophone (September, 2017). [Online]. Available: http://www.youtube.com/watch?v=tc82Z_yfEwc

[6] B. Chambayil, R. Singla, and R. Jha, *EEG Eye Blink Classification Using Neural Network*, Springer-Verlag Berlin Heidelberg, July 2, 2010, vol. 1, pp. 603-608.

[7] N. A. Chadwick, D. A. McMeekin, and T. Tan, “Classifying eye and head movement artifacts in EEG signals,” in *Proc. 5th IEEE International Conference on Digital Ecosystems and Technologies Conference*, 2011, pp. 285–291.

[8] A. N. Belkacem, H. Hirose, N. Yoshimura, D. Shin, and Y. Koike, “Classification of four eye directions from EEG signals for eye-movement-based communication systems,” *Journal of Medical and Biological Engineering*, vol. 34, no. 6, pp. 581-58, December 2014.

[9] Q. C. Lam, L. A. T. Nguyen, and H. K. Nguyen, “A novel approach for classifying EEG signal with multi-layer neural network,” in *Proc. 2nd International Conference on Mechanical Automation and Control Engineering*, January 5-7, 2018 (Accepted).

[10] A. Grant, J. A. Hinoojsa, and M. S. Oliveira, “Methods of eeg signal features extraction using linear analysis in frequency and time – Frequency Domains,” Hindawi Publishing Corporation ISRN Neuroscience, 2014, pp 1-7.

[11] Delta waves. (September, 2017), [Online]. Available: https://en.wikipedia.org/wiki/Delta_wave

[12] C. B. Rael and P. John, “Meditation states and traits: EEG, ERP, and neuroimaging studies,” *Psychological Bulletin*, vol. 132, no. 2, pp. 180–211, 2006.

[13] E. Niedermeyer, “Alpha rhythms as physiological and abnormal phenomena,” *International Journal of Psychophysiology*, vol. 26, no. 1–3, pp. 31–49, 1997.

[14] G. Pfurtscheller and F. H. L. da Silva, “Event-related EEG/MEG synchronization and desynchronization: Basic principles,” *Clinical Neurophysiology*, vol. 110, no. 11, pp. 1842–1857, 1999.

[15] E. Niedermeyer and F. L. da Silva, “Electroencephalography: Basic principles, clinical applications, and related fields,” *Lippincott Williams & Wilkins*, 2004.

[16] EEG Data. (September 2017). [Online]. Available: http://sccn.ucsd.edu/~arno/fam2data/publicly_available_EEG_data.html

[17] C. C. Lo, T. Y. I Chien, Y. C. Chen, S. H. Tsai, W. C. Fang, and B. S. Lin, “A wearable channel selection-based brain-computer interface for motor imagery detection,” *Sensors*, vol. 16, no. 2, 2016.

[18] A. Temko, G. Boylan, W. Marnane, and G. Lightbody “Robust neonatal EEG seizure detection through adaptive background modeling,” *Int. J Neural Syst.*, vol. 23, no. 4, pp. 1350018, 2013.

[19] P. Goupillaud, A. Grossmann, and J. Morlet, “Cycle-octave and related transforms in seismic signal analysis,” *Geoexploration*, vol. 23, no. 1, pp. 85–102, 1984.

[20] Y. Meyer, *Wavelets and Applications*, Paris: Masson; 1992.

[21] A. J. Casson, D. C. Yates, S. Patel, and E. Rodriguez-Villegas, “An analogue bandpass filter realisation of the continuous wavelet transform,” in *Proc. 29th Annual*

International Conference of the IEEE EMBS, Lyon, France August 23-26, 2007, pp. 1850-1854.

[22] J. I. Mwasiagi, X. H. Wang, and X. B. Huang, "The use of K-means and artificial neural network to classify cotton lint," *Fiber and Polymers*, no. 10, pp. 379–383, 2009.

[23] U. Orhan, M. Hekim, and T. Ibrikci, "Gravitational fuzzy clustering," *Lecture Notes in Artificial Intelligence*, no. 5317, pp. 524–531, 2008.

[24] S. O. Haykin, "Neural networks and learning machines," *Prentice Hall*, 2008.

[25] J. W. Han and M. Kamber, *Data Mining: Concepts and Techniques*, Second Edition, Elsevier Inc., All Rights Reserved, 2006.

[26] C. Willmott and K. Matsuura, "Advantages of the Mean Absolute Error (MAE) over the Root Mean Square Error (RMSE) in assessing average model performance," *Clim. Res.*, no. 30, pp. 79–82, 2005.

[27] R. Kohavi and F. Provost, *Glossary of Terms*, Editorial for the Special Issue on Applications of Machine Learning and the Knowledge Discovery Process, 1998.

Quang Chuyen Lam is the dean of electrical and electronic engineering faculty, Ho Chi Minh City Industry and Trade College, Vietnam. He received B.Sc. degree in electronic and M.Sc. degree in Automation. His current research interests include Electronic, Control Engineering and Automation. Currently, he is also Ph.D. student

Luong Anh Tuan Nguyen is the head of Information System Depatment, Ho Chi Minh City University of Transport, Vietnam. He received B.Sc. and M.Sc. in Computer Science from University of Science – Viet Nam National University Ho Chi Minh City. He also received Ph.D. degree in Control Engineering and Automation. His current research interests include Artificial Intelligence, Soft Computing, Control Engineering and Automation.

Huu Khuong Nguyen received Ph.D. degree in automation control engineering from the Russian Academy of Sciences in 1999. Since 2005, he has been an associate professor. He chaired a lot of research projects. He was former vice president of Ho Chi Minh City University of Transport, Vietnam. Currently, he is in charge of traffic electricity department. His research interests include Electronic, Control Engineering and Automation.